Journal of Theoretical and Applied Information Technology
15th March 2020. Vol.98. No 05

ISSN: 1992-8645 www.jatit.org E-ISSN: 1817-3195

AUTOMATED MALARIA DIAGNOSIS USING OBJECT DETECTION RETINA-NET BASED ON THIN BLOOD SMEAR IMAGE

JASMAN PARDEDE[1], IRMA AMELIA DEWI[2], REZA FADILAH[3], YANI TRIYANI[4]

[1,2,3]Department of Informatics, Institut Teknologi Nasional, Bandung, Indonesia

[4]Faculty of Medicine, Universitas Islam Bandung, Bandung, Indonesia

Email: [1]jasman@itenas.ac.id, [2]irma_amelia@itenas.ac.id, [3]rezafd23@gmail.com,

[4]ytriyani87@gmail.com

ABSTRACT

Malaria diagnosis is decided based on index malaria value which calculated from the amount of normal and infected erythrocyte on thin blood smear using microscope by a clinical pathologist. This activity is done manually and wastes a lot of time. Object detection using Convolutional Neural Network (CNN) is one of approach for solving this problem. However, the traditional object detection using CNN shows inadequate classification performance in labelling classes object. This paper is focused on the implementation of RetinaNet object detection approach to diagnose malaria. First, ResNet101 and ResNet50 used as RetinaNet backend network architecture for detecting both normal and infected erythrocytes on thin blood smear image with 1000x microscope zoom. Next, count every label of detected-object and calculate malaria-index value. Finally, after malaria-index value obtained, malaria diagnosis is defined. The algorithm performance with ResNet101 backend shows average precision (AP) 0,94, average recall 0,74, and average accuracy 0,73. Then the usage of ResNet50 backend in RetinaNet algorithm show average precision (AP) 0,90, average recall 0,78 and average accuracy 0,71.

Keywords: *Convolutional Neural Network, Object Detection, Deep Learning, Malaria Detection, Thin Blood Smear Image*

1. INTRODUCTION

Malaria is one of disease which caused by plasmodium parasite that infects red blood cells [1]. Reported by Indonesian ministry of health on malaria InfoDatin, east area of Indonesia, particularly Papua, still reported as endemic area of malaria or in other words, there still a lot of malaria cases in Papua [2]. But, the cases of malaria still occur in non-endemic malaria area such as west java. One of malaria diagnosis procedure is laboratory test on red blood cells of a patient [3]. The laboratory test done on thin blood film which created from blood cells sample of patient that put on the blood film and Giemsa staining. Furthermore, the clinical pathologist calculates the index malaria value from infected and normal founded erythrocytes using microscope manually. Based on Soergadegar research about automated *parasitemia* counting in [4], counting the number of erythrocytes is time-consuming activity. If the expert found the infected erythrocyte, then the patient diagnosed malaria.

Object detection approach focuses not only on labelling different images but also try to define the form and locate the object precisely in each image [5]. The number of dataset and variant of dataset in training object detection may affect the system in recognizing the object and the location of object in each image. Big amount and more variance dataset can make the system more precisely detecting the target object and both factors may reduce the *over-fitting*. The other necessary component of object detection such as feature detector, hypothesis formation and hypothesis verification must be contained in a system [5]. Object detection framework divided into two categories. First category is region proposed based framework [5] such as RCNN, Fast R-CNN [7], Faster R-CNN [8], FPN [9], and Mask R-CNN [10]. Second category is classification-based framework [5] such as Yolo [11] and SSD [12]. Region based framework better in detecting every single object precisely, but the weakness is this method take a lot of time for define every object. On the other hand, the classification

ISSN: 1992-8645 www.jatit.org E-ISSN: 1817-3195

framework performance in detection object is not good enough as region proposed framework, but the time required is no long as region proposed framework need. Both techniques have pros and cons. Moreover, there is a hybrid model which designed by combine both FPN as feature extractor and classification based framework technique to define the bounding box and label of object called RetinaNet [12]. RetinaNet also use focal loss as loss function to minimize the loss information during training process. Most of object detection with deep learning approach use Convolutional Neural Network (CNN) used as feature detector or feature extractor in this approach [13].

A lot of deep learning CNN methods are implemented on medical field to identify cell object or bacterial counting. Deep CNN is implemented in [14] for counting bacteria colonies on microbiological plates. In malaria field, two papers implemented deep learning approaches to identify malaria. Deep CNN [15] used thick blood smear identifier to diagnose malaria. [4] implements R-CNN for identify the normal and infected erythrocytes on thin blood smear image then count the index value of malaria using smartphone camera. Faster R-CNN is implemented in [16] for detecting type of *plasmodium vivax* which infected red blood cell and leukocyte from thin blood smear image.

From [4] research, the R-CNN performance of classifying object is inadequate performance and counting *parasitemia* is time-consuming activity. This paper is motivated by those problems to implement RetinaNet object detection to identify erythrocytes object and diagnose malaria.

This paper is organized as follows: an introduction in section 1. The previous work of related topics presented in section 2. The state-of-the-art of this work described in section 3. Section 4 described the experimental result from the state-of-the-art. To conclude all section, section 5 explain the conclusion of this paper.

2. RELATED WORK

The previous work about malaria done by Zhang et al. [17] introduced robust template of infected and normal erythrocytes classification. Histogram of Oriented Gradient (HOG) used as a feature extractor from the template and Viola-Jones object detection framework is used for detecting normal, infected red blood cells, and image background. Later, Quinn et al. [15] implement deep convolutional neural network architecture for diagnosing malaria based on thick blood smear image, tuberculosis in sputum samples, and intestinal parasite eggs in stool samples. Quinn et. al research diagnose malaria by detecting Plasmodium from thick blood film images which taken from dedicated microscope camera. Poostchi et al. [18] try to exploration in detecting malaria from thin and thick blood smear image with a lot of configuration algorithms. Poostchi et al divide their research into pre-processing, segmentation, and classification parts. Each part contains with some algorithm techniques. For example, wavelet transform, gradient texture, Fractal, etc. used in pre-processing part. Then, feature extraction based on color, texture, and morphologic are applied in each image. Supervised learning such as bayesian classifier, naïve bayes tree [19], k-nearest neighbors classifier [20], linear discriminant (LD) [21], support vector machine (SVM) [22],[23], normalized cross-correlation [24], deep learning approach [25],[26], [27],[28], etc.

Recently, another deep learning methods such R-CNN applied on automated *parasitemia* counting by Sorgedrageron his paper [4]. Sorgedrager implements R-CNN with improvement in feature extraction parts by splitting every object in images into small pieces then classify them into healthy and infected erythrocytes. The research done with low resolution image that taken from smartphone camera and the experimental result of the method compared with 2 experts. Moreover, Faster R-CNN method is applied by Hung et.al [16] on detecting the types of *plasmodium vivax* on red blood cells and leukocyte objects based on thin blood smears image.

This paper implements the novel object detection techniques RetinaNet on malaria diagnosis based on thin blood smear images.

3. APPROACH

Figure 1 shows the block diagram of overall framework in this research. Standard RetinaNet state-of-the-art applied in this paper. Figure 2 which taken originally from [12]. It describes the general RetinaNet state-of-the-art. In the training process part, each data training labelled with ***LabelImg*** in every erythrocytes object for both normal and infected erythrocytes then save the label in xml format, then convert the *.xml file into *.csv file. Every data training will firstly preprocessing using image data generator function from *Keras* such as random flip, rotate, and dilatation. Then every erythrocytes object in each image will be extracted by residual model CNN of ResNet101 and ResNet50 backend in 100 epochs which shown in part a of Figure 2. Then the feature of every object will be created as feature pyramid network which shown in

Journal of Theoretical and Applied Information Technology
15th March 2020. Vol.98. No 05

ISSN: 1992-8645 www.jatit.org E-ISSN: 1817-3195

part b of Figure 2. The detail of residual model process is drawn in Figure 3 which taken from [29]. After the feature of each object extracted, the loss function will be calculated for every class of label with focal loss function in this following equation. Based on [12], α=0,25 and γ=2.

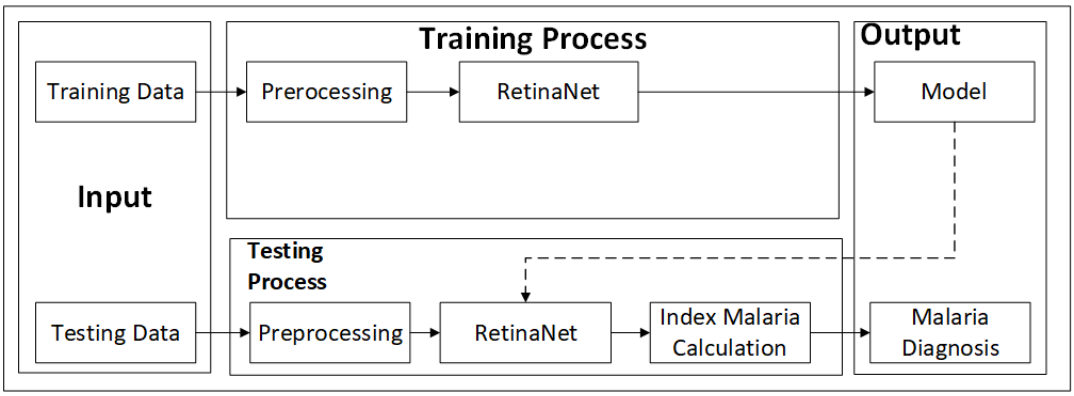

Figure 1 Block Diagram of the Research

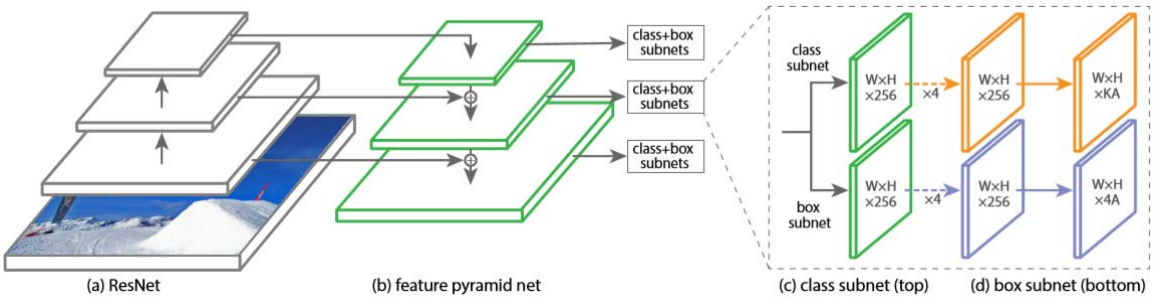

Figure 2 State-of-the-art RetinaNet

$$FL(p_t) = -\alpha(1-p_t)^{\gamma}\log(p_t) \ldots\ldots (1)$$

In the testing part of the system, firstly pre-processing is done with each testing image by extract the ImageNet mean [30]. Every RGB matrix image will be extracted then convert the matrix into BGR type and reduced by caffe mode filter with this following equation.

$$B\,[\ldots,0] -= 103{,}939$$
$$G\,[\ldots,1] -= 116{,}779 \ldots\ldots\ldots\ldots (2)$$
$$R\,[\ldots,2] -= 123{,}68$$

Futhermore, the extracted feature of image done in each pre-processing result image by FPN with ResNet101 and ResNet50 backend. The output from feature extraction are P_3 – P_7 pyramid of FPN. Parallel process such labelling in classification subnet and creating fixed bounding box in box-regression subnet applied on the result of feature extraction. Classification subnet contain simple fully connected network (FCN) which applies four 3x3 convolution on pyramid feature result from feature extraction with C channels followed by ReLU activation. Then,3x3 convolution with K A filters applied on the previous result. As default of RetinaNet architecture the value of C=256 and A=9. In box regression subnet, simple FCN as FCN in classification subnet applied on each pyramid level for the purpose of regressing the offset from each

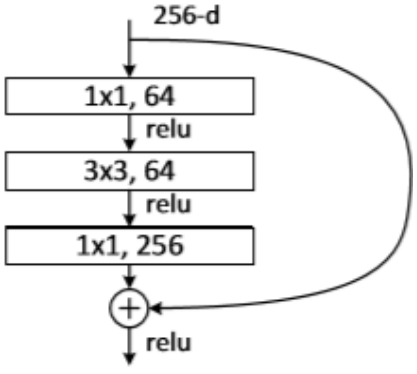

Figure 3 Residual Model

anchor box to a nearby ground-truth object. To improve the prediction speed, predicted box is applied on 1000 top-scoring box in each FPN level and to get final prediction of the bounding box, all prediction in each FPN level combined with non-maximum suppression with 0,5 threshold.

ISSN: 1992-8645 www.jatit.org E-ISSN: 1817-3195

Finally, to calculate the malaria index value equation (3) applied in this paper.

$$index\ malaria = \frac{x}{y} x100\% \text{ ..... (3)}$$

The value of x in equation (3) is the number of infected erythrocytes, and y is the number of normal and infected erythrocytes from detected erythrocytes object in testing image. If the index value more than 0%, then the diagnosis of patient is malaria.

4. RESULTS

In this section, this paper compares the performance of RetinaNet state-of-the-art with ResNet101 and ResNet50 backend. This method is implemented in two machines. First machine which used for training the data has Xeon processor, 64 GB RAM, Nvidia Tesla V100, and 100 GB SSD specification form floydhub.com server. The second machine that used for testing the model has i7 4720HQ, 12 GB RAM, Nvidia Geforce 940M, and 256 GB SSD specification. The experiment uses Tensorflow and Keras for implementing RetinaNet model.

4.1 Dataset

This research uses dataset image from [16] and Dr Yani Triyani repositories. This dataset contains 25 images for testing and 2 images for training from [16],75 images for testing and 4 images for training from Dr. Yani Triyani. The amount of training data is 255 objects which divided into 2 classes label, Normal and Infected erythrocytes. Each image has varied size. Testing dataset are divided into 2 parts testing. First part of testing is done with 75 images which contain infected and normal erythrocytes in each image. Second part of testing is done with 25 images which contain normal erythrocytes to test the system in testing normal erythrocytes. Some examples of training data are shown in Figure 4 and Figure 5. The detail example of Normal erythrocyte is shown in Figure 6 and infected erythrocytes is shown in Figure 7.

4.2 Evaluation Criterion

To evaluate the method performance in both ResNet50 and ResNet101 backend in RetinaNet model, this paper uses precision, recall, and accuracy to get quantitative value of evaluation. Precision, recall, and accuracy evaluation is one of image field evaluation either machine learning, deep learning, or information retrieval [31][32][33]. Precision is defined as how relevant the algorithm or a method predict the object, recall is defined as how the algorithm can retrieve the object, while accuracy is defined as the correctness of classification object [32].

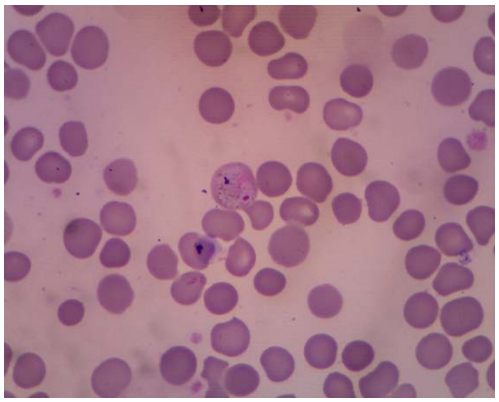

Figure 4 Example of Training Data from Dr Yani Triyani Repositories

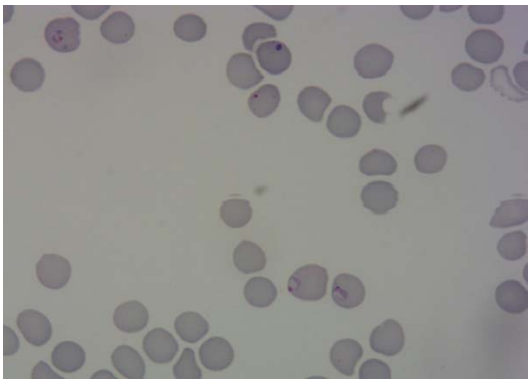

Figure 5 Example of Training Data from Hung et.al Research

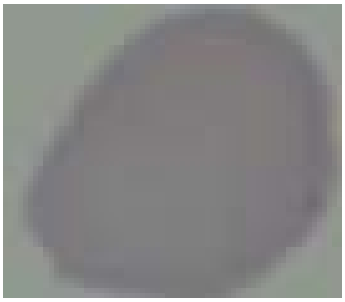

Figure 6 Normal Erythrocytes

ISSN: 1992-8645 www.jatit.org E-ISSN: 1817-3195

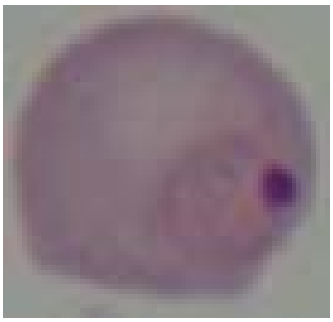

Figure 7 Infected Erythrocytes

4.3 Training

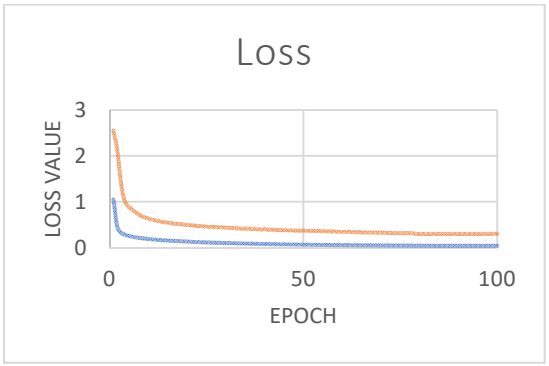

Figure 8 Loss Graph Value

The model used in this paper is based on custom training with 255 objects data training without using pre-trained model. The model is built with 100 epoch and 16 batch size training setting for both ResNet50 and ResNet101 backend. From 100 epoch training, RetinaNet model with ResNet101 backend shows 0,0398 classification loss and 0,2986 regression loss while ResNet50 backend shows 0,0461 classification loss and 0,316 regression loss. Figure 8 illustrates the graph of resulted loss value during training. The training of RetinaNet with ResNet101 backend done in 28 hours while RetinaNet with ResNet50 backend done in 23 hours.

4.4 Experimental Result

To give rich information about implementation of RetinaNet object detection in malaria cases, this paper compares RetinaNet with ResNet101 and ResNet50 backend in detecting malaria from thin blood smear images. The comparison based on 100x testing which divided into 3 categories testing. In the first testing, 50 images which contain infected and normal erythrocytes object in each image from [14]. The second testing used 50 images which contain both infected and normal erythrocytes from Dr Yani Triyani repositories, and the third testing is a particular testing to test the system in detecting normal erythrocytes with 25 images from Dr Yani Triyani repositories. From the first and second testing, both model of system can calculate the malaria index value and decide the malaria diagnosis based on index value which obtained from normal and infected erythrocytes object in each image.

In Table 1 and Table 2 shows the 10 example results of first and second testing compare with the doctor result which determined as ground truth value. In both tables, the result of the testing with ResNet101 and ResNet50 backend of RetinaNet model show various difference of detected objects and index value comparing to the doctor result. Both models show the difference results either. The diversity result of the model can be affected by difference layer of the the backend, then every model extracts the different features of every object in each image, from that different feature the system decides the different predict object. In Figure 9 and Figure 10 illustrates the one of identification result in first parts testing with ResNet101 and ResNet50 on RetinaNet model. Additionally, in Figure 11 and Figure 12 describes the one of identification result in second parts testing with ResNet101 and ResNet50 on RetinaNet model

Table 1 10 Samples of Detection Result from Hung et.al Testing Images

Images	Normal			Infected			Index Value			Diagnosis
	A	B	D	A	B	D	A	B	D	
4	18	19	24	3	5	1	15%	21%	4%	Infected Malaria
5	16	17	58	3	2	3	16%	11%	5%	Infected Malaria
6	13	13	54	5	5	6	28%	28%	10%	Infected Malaria
7	16	10	40	4	8	4	20%	44%	9%	Infected Malaria
8	9	18	58	2	2	2	18%	10%	3%	Infected Malaria
9	7	20	41	5	4	3	42%	17%	7%	Infected Malaria
12	38	38	49	1	1	2	3%	3%	4%	Infected Malaria
13	15	20	35	6	1	1	29%	5%	3%	Infected Malaria
14	22	18	33	3	5	1	12%	22%	3%	Infected Malaria
15	31	29	34	1	3	1	3%	9%	3%	Infected Malaria

ISSN: 1992-8645 www.jatit.org E-ISSN: 1817-3195

5 sample results of the third testing are shown in Table 3. Within 25 image testing, both models successfully detect normal erythrocytes object, but in some images, there are miss-prediction object done by both models. Figure13 shows the example of the third testing result with miss-prediction.

Red box on Figure 9 – Figure 13 show the normal erythrocytes and orange box show the infected erythrocytes. Then, label A in Table 1-3 means the result of RetinaNet model with ResNet101 backend, Label B means the result of RetinaNet model with ResNet50 backend and D means the result of doctor identification.

Table 2 10 Samples of Detection Result from Dr Yani Triyani Testing Images

Images	Normal			Infected			Index Value			Diagnosis
	A	B	D	A	B	D	A	B	D	
74	50	51	50	3	2	1	6%	4%	1,96%	Infected Malaria
75	55	56	58	1	2	1	2%	3%	1,69%	Infected Malaria
76	49	40	52	2	4	1	4%	9%	1,89%	Infected Malaria
77	46	44	50	5	5	2	10%	10%	3,85%	Infected Malaria
78	51	49	50	10	3	11	16%	6%	18,03%	Infected Malaria
79	49	58	62	3	3	1	6%	5%	1,59%	Infected Malaria
80	38	50	68	8	3	3	17%	6%	4,23%	Infected Malaria
81	37	51	61	10	2	2	21%	4%	3,17%	Infected Malaria
82	39	43	43	15	12	14	28%	22%	24,56%	Infected Malaria
83	26	17	33	12	19	14	32%	53%	29,79%	InfectedMalaria

Table 3 Sample of Normal Detection Results

Images	A	B	D
1	85	87	83
2	89	94	81
3	77	78	74
4	103	110	97
5	82	78	88

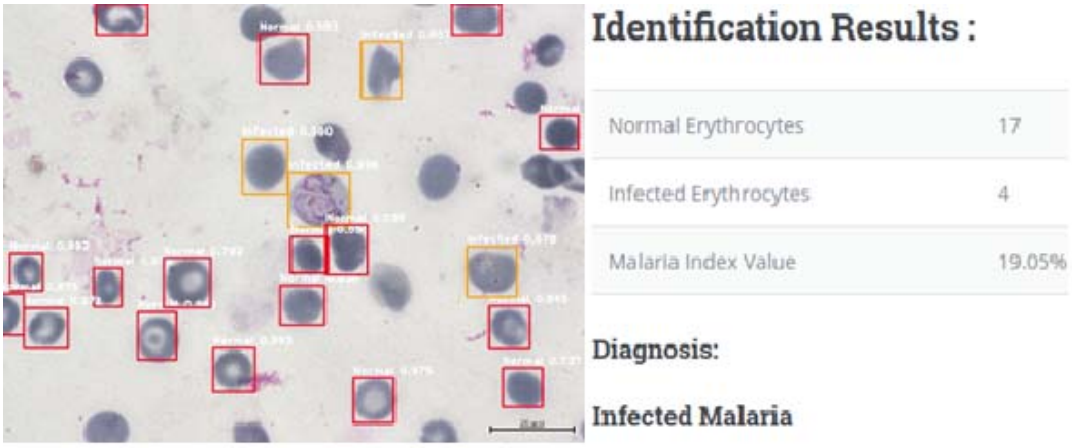

Figure 9 RetinaNet with ResNet101 Backend Identification Result on Hung et.al Testing Image

ISSN: 1992-8645 www.jatit.org E-ISSN: 1817-3195

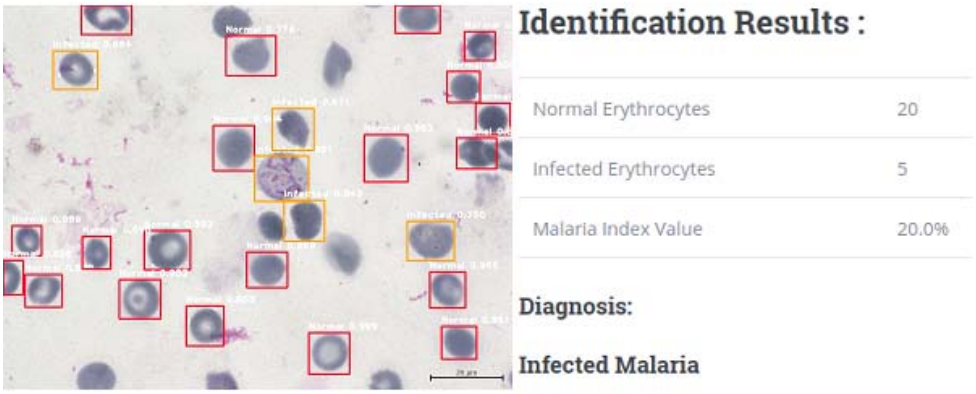

Figure 10 RetinaNet with ResNet50 Backend Identification Result on Hung et.al Testing Image

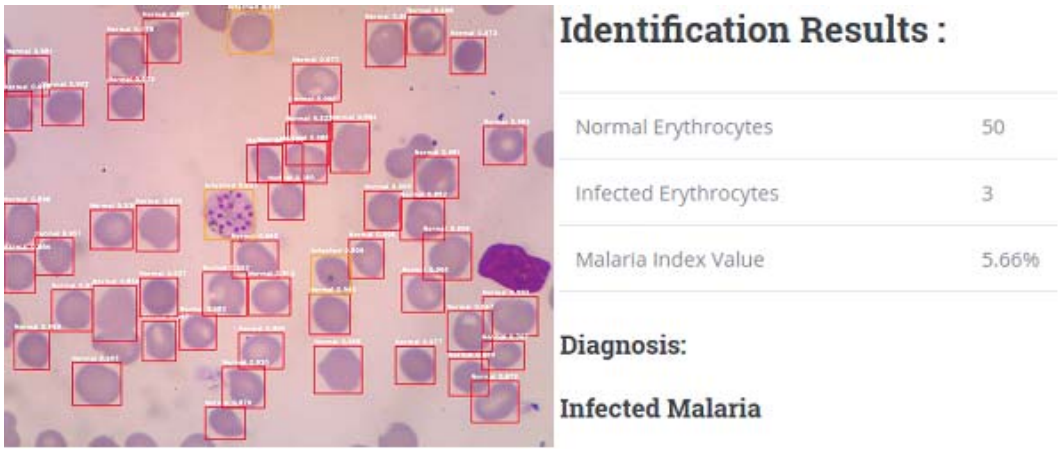

Figure 11 RetinaNet with ResNet101 Backend Identification Result on Dr YaniTriyani Repositories Testing Image

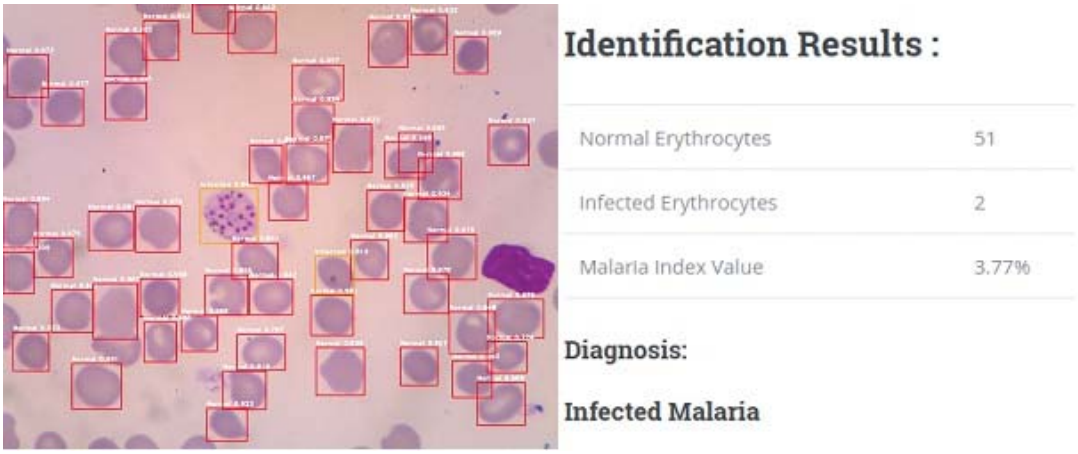

Figure 12 RetinaNet with ResNet50 Backend Identification Result on Dr YaniTriyani Repositories Testing Image

ISSN: 1992-8645 www.jatit.org E-ISSN: 1817-3195

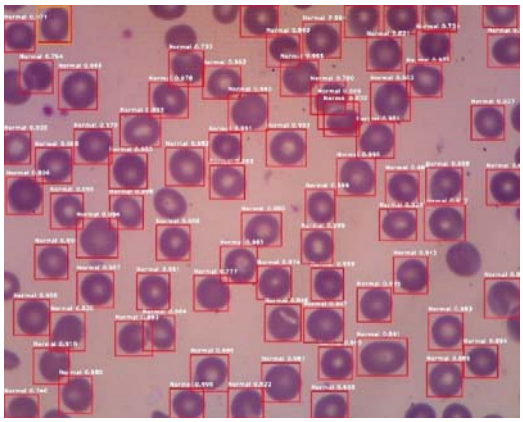

Figure 13 Misspredict Label Example

To give measurable RetinaNet performance in detecting erythrocytes object, Table 4 shows average result of precision, recall, and accuracy value within erythrocytes detection by RetinaNet model with ReNet101 and ResNet50 backend. A model with ResNet101 backend gives a better result in precision with 0,94 value than [4] in detecting erythrocytes object. Recall and accuracy values of both models shows inadequate performance. RetinaNet with ResNet101 backend gives 0,74 recall and 0,73 accuracy and ResNet50 backend in RetinaNet model gives 0,78 recall and 0,71 accuracy. This can be due to small amount of training data while creating the model. Then, every model predicts the various erythrocytes object not optimally. Small amount of training data caused by financial issue for renting the floydhub.com server. To give easy reading, Figure 14 illustrates the chart of precision, recall, and accuracy in erythrocytes detection.

On the other hand, this paper also evaluates the model in classifying normal and infected erythrocytes within precision, recall, and accuracy value. Table 5 informs the average result of giving normal label in erythrocytes object during testing and Figure 15 illustrates the chart of classifying normal erythrocytes performance. Both backend in RetinaNet models show satisfied performance in labelling normal erythrocytes. RetinaNet with ResNet101 backend shows 1,0 precision, 0,98 recall and 0,98 accuracy while RetinaNet with ResNet50 shows 0,99 precision, 1,0 recall, and 1,0 accuracy. In evaluating of infected labelling within erythrocytes object, Table 6 shows the average precision, recall, and accuracy in labelling infected erythrocytes. Both back-ends in RetinaNet model give inadequate precision result and better result in recall and accuracy side. RetinaNet with ResNet101 backend gives 0,67 precision, 1,0 recall, and 0,99 accuracy. Moreover, RetinaNet with ResNet50 backend gives 0,64 precision and 1,0 of recall and accuracy. In Figure16, shows the graph of average precision, recall, and accuracy of RetinaNet model with both backend.

Table 4 Evaluation Result of Erythrocytes Detection

Evaluation	ResNet101			ResNet50		
	Precision	Recall	Accuracy	Precision	Recall	Accuracy
1	0,92	0,53	0,56	0,84	0,64	0,56
2	0,94	0,85	0,80	0,92	0,81	0,75
3	0,96	0,85	0,82	0,95	0,88	0,83
Average	0,94	0,74	0,73	0,90	0,78	0,71

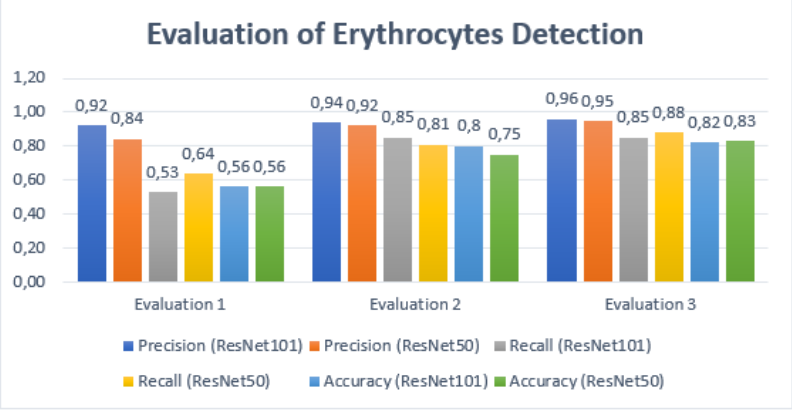

Figure 14 Graph of Evaluation Erythrocytes Detection

ISSN: 1992-8645 www.jatit.org E-ISSN: 1817-3195

Table 5 Evaluation Result of Labelling Normal Erythrocytes

Evaluation	ResNet101			ResNet50		
	Precision	Recall	Accuracy	Precision	Recall	Accuracy
1	1,00	0,96	0,96	0,99	1,00	1,00
2	1,00	1,00	1,00	0,99	1,00	1,00
3	0,99	0,99	0,99	0,99	0,99	0,99
Average	1,00	0,98	0,98	0,99	1,00	1,00

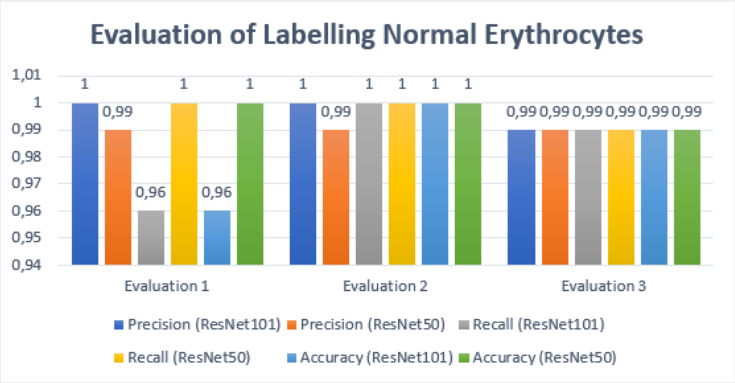

Figure 15 Graph of Evaluation Labelling Normal Erythrocytes

Table 6 Evaluation Result of Labelling Infected Erythrocytes

Evaluation	ResNet101			ResNet50		
	Precision	Recall	Accuracy	Precision	Recall	Accuracy
1	0,71	0,99	0,98	0,66	1,00	1,00
2	0,62	1,00	1,00	0,62	1,00	1,00
Average	0,67	1,00	0,99	0,64	1,00	1,00

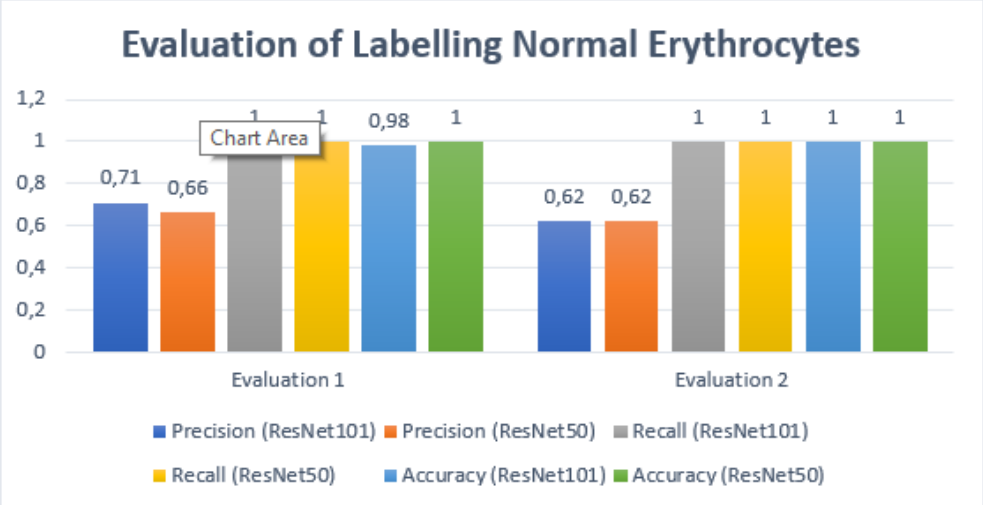

Figure 16 Graph of Evaluation Labelling Infected Erythrocytes

5. CONCLUSIONS

In this paper, RetinaNet object detection approach is applied for diagnosing malaria based on thin blood smear image with ResNet101 and ResNet50 backend. Based on third evaluation with 100 images, RetinaNet with both ResNet101 and ResNet50 backend show the adequate performance in detecting erythrocytes object and labelling normal erythrocytes. But in labelling infected erythrocytes this model performs inadequate with low score of precision value. This can be due to small amount and

ISSN: 1992-8645 www.jatit.org E-ISSN: 1817-3195

variation of infected erythrocytes data training. However, both back-ends of RetinaNet model can successfully diagnose malaria. Thus, for improving the the performance of RetinaNet model in identifying malaria object from erythrocytes, enlarging the amount of training data must be tried.

REFRENCES

[1] K. Plewes, S. J. Leopold, H. W. Kingston and A. M. Dondorp, "Malaria: What's New in the Management of Malaria?," Infectious Disease Clinics of North America, vol. 33, no. 1, pp. 39-60, 2019.

[2] K. R. "InfoDatin Malaria," Pusdatin Kementrian Kesehatan RI, 2016.

[3] E. Sariwati, Buku Saku Penatalaksanaan Kasus Malaria, Jakarta: Kementrian Kesehatan Republik Indonesia, 2017.

[4] R. Sorgedrager, "Automated malaria diagnosis using convolutional neural networks in an on-field setting," Delft Center for Systems and Control, Delft, 2018.

[5] Z.-Q. Zhao, P. Zheng, S.-t. Xu and W. Xindong , "Object Detection with Deep Learning: A Review," Computer Vision and Pattern Recognition, 2019.

[6] R. Girshick , "Fast R-CNN," IEEE, pp. 1440-1448, 2015.

[7] S. Ren, K. He, R. Girshick and J. Sun, "Faster R-CNN: Towards Real-Time Object Detection with Region Proposal Networks," Computer Vision and Pattern Recognition Cornell University, 2016.

[8] T.-Y. Lin, . P. Dollár, R. Girshick, K. He, B. Hariharan and S. Belongie, "Feature Pyramid Networks for Object Detection," Computer Vision Foundation (CVF), pp. 2118-2125, 2016.

[9] K. He, G. Gkioxari , P. Dollár and R. Girshick, "Mask R-CNN," Computer Vision and Pattern Recognition Cornell University, 2017.

[10] J. Redmon, S. Divvala, R. Girshick and A. Farhadi, "You Only Look Once: Unified, Real-Time Object Detection," CVPR, 2016.

[11] W. Liu, D. Anguelov, D. Erhan, C. Szegedy, S. Reed, F. Cheng-Yang and A. C. Berg, "SSD: Single Shot MultiBox Detector," CVPR, 2016.

[12] T.-Y. Lin, P. Goyal, R. Girshick, . K. He and P. Dollár, "Focal Loss for Dense Object Detection," Computer Vision and Pattern Recognition, 2017.

[13] M. Alaslani and L. Elrefaei, "CONVOLUTIONAL NEURAL NETWORK BASED FEATURE EXTRACTION FOR IRIS RECOGNITION," International Journal of Computer Science & Information Technology (IJCSIT), vol. 10, pp. 65-78, 2018.

[14] A. Ferrari, S. Lombardi and A. Signoroni, "Bacterial Colony Counting with Convolutional Neural Networks in Digital Microbiology Imaging," Pattern Recognition , pp. 629-640, 2016.

[15] J. A. Quinn, R. Nakasi, P. K. B. Mugagga, B. Patrick , W. Lubega and A. Andama, "Deep Convolutional Neural Networks for Microscopy-Based Point of Care Diagnostics," Computer Vision and Pattern Recognition Cornell University, 2016.

[16] J. Hung, D. Ravel, S. C. Lopes, G. Rangel, O. A. Nery, B. Malleret, F. Nosten, M. V. G. Lacerda, M. U. Ferreira, L. Rénia, M. T. Duraisingh, F. T. M. Costa, M. Marti and A. E. Carpenter, "Applying Faster R-CNN for Object Detection on Malaria Images," Computer Vision and Pattern Recognition, 2018.

[17] Z. Zhang, L. S. Ong, K. Fang, A. Matthew, J. Dauwels, M. Dao and H. Asada, "Image classification of unlabeled malaria parasites in red blood cells," in 38th Annual International Conference of the IEEE Engineering in Medicine and Biology Society (EMBC), Orlando, FL, USA, 2016.

[18] M. Poostchi, K. Silamut, R. J. Maude, S. Jaeger and G. Thoma, "Image analysis and machine learning for detecting malaria," Translational Research, vol. 194, pp. 36-55, 2018.

[19] D. Das, M. A. K and C. C, "Automated system for characterization and classification of malaria-infected stages using light microscopic images of thin blood smears," Journal of Microscopy, pp. 257(3):238-52, 2015.

[20] A. Nanoti, S. Jain, C. Gupta and G. Vyas, "kNN classification based erythrocyte separation in microscopic images of thin blood smear," in International Conference on Inventive Computation Technologies (ICICT), Coimbatore, India, 2016.

[21] H. S. Park, M. T. Rinehart, K. A. Walzer, J.-T. A. Chi and A. Wax, "Automated Detection of P. falciparum Using Machine Learning

ISSN: 1992-8645 www.jatit.org E-ISSN: 1817-3195

Algorithms with Quantitative Phase Images of Unstained Cells," Plos One, p. 11(9):e0163045, 2016.

[22] D. Yang, G. Subramanian, J. Duan, S. Gao, L. Bai, R. Chandramohanadas and Y. Ai, "A portable image-based cytometer for rapid malaria detection and quantification," Plos One, p. 12(6): e0179161., 2017.

[23] A. Nanoti, S. Jain, C. Gupta and G. Vyas, "Detection of malaria parasite species and life cycle stages using microscopic images of thin blood smear," in International Conference on Inventive Computation Technologies (ICICT), Coimbatore, India, 2016.

[24] H. A. Mohammed and I. A. M. Abdelrahman, "Detection and classification of malaria in thin blood slide images," in International Conference on Communication, Control, Computing and Electronics Engineering (ICCCCEE), Khartoum, Sudan, 2017.

[25] D. Bibin, M. S. Nair and . P. Punitha, "Malaria parasite detection from peripheral blood smear images using deep belief networks," IEEE Access, vol. 5, pp. 9099-9108, 2017.

[26] Y. Dong, Z. Jiang, H. Shen, W. D. Pan, L. A. Williams, V. V. B. Reddy, W. H. Benjamin and A. W. Bryan, "Evaluations of deep convolutional neural networks for automatic identification of malaria infected cells," in IEEE EMBS International Conference on Biomedical & Health Informatics (BHI), Orlando, FL, USA, 2017 .

[27] G. . P. Gopakumar, M. Swetha, G. S. Siva and G. R. K. S. Subrahmanyam, "Convolutional neural network-based malaria diagnosis from focus stack of blood smear images acquired using custom-built slide scanner," Journal of Biophotonics, vol. 11, no. 3, 2017.

[28] Y. Dong, Z. Jiang, H. Shen and W. D. Pan, "Classification accuracies of malaria infected cells using deep convolutional neural networks based on decompressed images," in SoutheastCon, Charlotte, NC, USA, 2017.

[29] K. He, X. Zhang, . S. Ren and J. Sun, "Deep Residual Learning for Image Recognition," in IEEE Conference on Computer Vision and Pattern Recognition (CVPR), Las Vegas, 2016.

[30] Fizyr, "Keras-retinanet," 24 November 2018. [Online]. Available: https://github.com/fizyr/keras-retinanet. [Accessed 20 June 2019].

[31] C. D. Manning, P. Raghavan and H. Schütze, An Introduction to Information Retrieval, Cambridge: Cambridge University Press, 2009.

[32] J. Pardede, M.G. Husada, "Comparison of VSM, GVSM, and LSI in Information Retrieval for Indonesian Text", Journal Teknologi, vol.78, no. 5-6, pp.51-56, 2016.

[33] J. Pardede, M.M. Barmawi, "Implementation of LSI Method on Information Retrieval for Text Document in Bahasa Indonesia", Internetworking Indonesia Journal, vol.8, no. 1, pp.83-87, 2016.